Stereochemically Dynamic 2,2′-Biphosphole Ligands for Asymmetric Catalysis

Emmanuel Robé,[†] Carmen Ortega,[†,§] Maciek Mikina,[‡] Marian Mikolajczyk,[‡] Jean-Claude Daran,*[,†] and Maryse Gouygou*[,†]

Laboratoire de Chimie de Coordination, CNRS, 205 Route de Narbonne, F-31077 Toulouse Cedex, France, and Centre of Molecular and Macromolecular Studies, Polish Academy of Sciences, 90-363 Lodz, Sienkiewicza 112, Poland

Received May 9, 2005

The stereochemically dynamic 2,2′-biphospholes **8**, **9**, and **10** have been synthesized by asymmetric alkylation of 2,2′-biphospholyl anion with enantiomerically pure diol ditosylates. A good carbon-to-phosphorus induction has been obtained in particular in the case of compound **8**. The introduction of a chiral linker between the two phosphorus atoms resulted in partial chirality control of the central and axial chiralities of the 2,2′-biphosphole framework, as three diastereoisomers **a**, **b**, and **c** are obtained among the six expected. In solution at room temperature **a**, **b**, and **c** diastereoisomers exist as an equilibrium mixture; the interconversion occurred by phosphorus-inversion inducing atropoinversion. Reaction of the equilibrium mixture of 2,2′-biphosphole with $[MCl_2(CH_3CN)_2]$ resulted in dynamic resolution leading to diastereo- and enantiopure Pd- and Pt-complexes. Palladium-catalyzed asymmetric allylic substitution can be achieved with the ligands **8** and **10** with high activities but still moderate enantioselectivities.

Introduction

Advances in the area of transition metal-catalyzed asymmetric synthesis[1] have been traditionally guided by the concept that stereochemically rigid enantiopure ligands are required to achieve high enantioselectivities. Among these chiral ligands, diphosphanes played a dominant role, although their syntheses and resolution are difficult because of racemization at higher temperature.[2]

A conceptually new strategy for asymmetric catalysis consists in the use of stereochemically dynamic ligands rather than the use of classical stereochemically rigid enantiopure ligands.[3] In this approach an enantiopure ligand (L*), sometimes referred to as a chiral activator, interacts with an achiral or meso ligand (L) and causes the latter to preferentially adopt one of its chiral conformations which is ultimately responsible for the transmission of asymmetry in enantioselective transformation. Successful results have been obtained with chirally flexible diphosphanes such as BIPHEP,[4] DPPF,[5] or NUPHOS.[6] This approach to asymmetric catalysis by direct use of this type of ligands without asymmetric synthesis or resolution clearly presents economical and environmental advantages.

In 1994, we began to focus our attention on a C_2-symmetric diphosphane combining central and axial chiralities: the 1,1′-diphenyl-3,3′,4,4′-tetramethyl-2,2′-biphosphole (BIPHOS). This diphosphane is a chirally flexible ligand because of the configurational instability of the axial chirality generated by the 2,2′-biphosphole framework and of the central chiralities at the phosphorus atoms.[7] The use of the stereochemically dynamic 2,2′-biphosphole (BIPHOS), after spontaneous resolution by crystallization and complexation on the Pd center, proved to be as effective as well-known chirally rigid diphosphines in asymmetric allylic substitution.[8]

As part of our continuing interest in chiral 2,2′-biphosphole ligands, we have explored a new approach to enantiopure 2,2′-biphosphole compounds as asymmetric ligands and catalysts. This approach is based on the facile isomerization of 2,2′-biphosphole to accomplish a dynamic resolution. Recently, we have reported preliminary results on metal dynamic resolution leading

* Corresponding authors. Tel: (33) 5 61 33 31 74. Fax: (33) 5 61 55 30 03. E-mail: daran@lcc-toulouse.fr; gouygou@lcc-toulouse.fr.
† Laboratoire de Chimie de Coordination.
‡ Centre of Molecular and Macromolecular Studies.
§ Present address: Dpto. de Química Orgánica, Facultad de Química, Circuito exterior s/n, Ciudad Universitaria, Coyoacán 04510, México.

(1) Ojima, I. *Catalytic Asymmetric Synthesis*, 2nd ed.; Wiley-VCH: New York, 2000. (b) Jacobsen, E. N.; Pfaltz, A.; Yamamoto, H. *Comprehensive Asymmetric Catalysis*; Springer-Verlag: Berlin, 1999. (c) Noyori, R. *Asymmetic Catalysis in Organic Synthesis*; Wiley: New York, 1994.

(2) (a) Pietrusiewicz, K. M.; Zablocka, M. *Chem. Rev.* **1994**, *94*, 1375−1411. (b) Valentine, D., Jr. *Asymmetric Synthesis*; Academic Press Inc.: New York, 1984; Vol. 4, pp 227−312.

(3) (a) Walsh, P. J.; Lurain, A. E.; Basells, J. *Chem. Rev.* **2003**, *103*, 3297−3344. (b) Mikami, K.; Aikawa, K.; Yusa, Y.; Jodry, J. J.; Yamanaka, M. *Synlett.* **2002**, *10*, 1561−1578, and references therein.

(4) (a) Mikami, K.; Kataoka, S.; Yusa, Y.; Aikawa, K. *Org. Lett.* **2004**, *6*, 3699−3701. (b) Mikami, K.; Aikawa, K.; Yusa, Y.; Hatano, M. *Org. Lett.* **2002**, *4*, 91−94. (c) Becker, J. J.; White, P. S.; Gagné M. R. *J. Am. Chem. Soc.* **2001**, *123*, 9478−9479. (d) Mikami, K.; Korenaga, T.; Terada, M.; Ohkuma, T.; Pham, T.; Noyori, R. *Angew. Chem., Int. Ed. Engl*. **1999**, *38*, 495−497.

(5) Mikami, K.; Aikawa, K. *Org. Lett.* **2002**, *4*, 99−101.

(6) (a) Doherty, S.; Knight, J. G.; Hardacre, C.; Luo, H.; Newman, C. R.; Rath, R. K.; Campbell, S.; Nieuwenhuyzen, M. *Organometallics* **2004**, *23*, 6127−6133. (b) Doherty, S.; Newman, C. R.; Rath, R. K.; Luo, H.; Nieuwenhuyzen, M.; Knight, J. G. *Org. Lett.* **2003**, *5*, 3863−3866.

(7) Tissot, O.; Gouygou, M.; Daran, J.-C.; Balavoine, G. G. A. *Chem. Commun.* **1996**, 2287−2288.

(8) Tissot, O.; Gouygou, M.; Dallemer, F.; Daran, J.-C.; Balavoine, G. G. A. *Angew. Chem., Int. Ed.* **2001**, *40*, 1076−1078.

10.1021/om0503646 CCC: $30.25
Publication on Web 10/01/2005

Scheme 1. Synthesis of the 2,2′-Biphosphole Derivatives

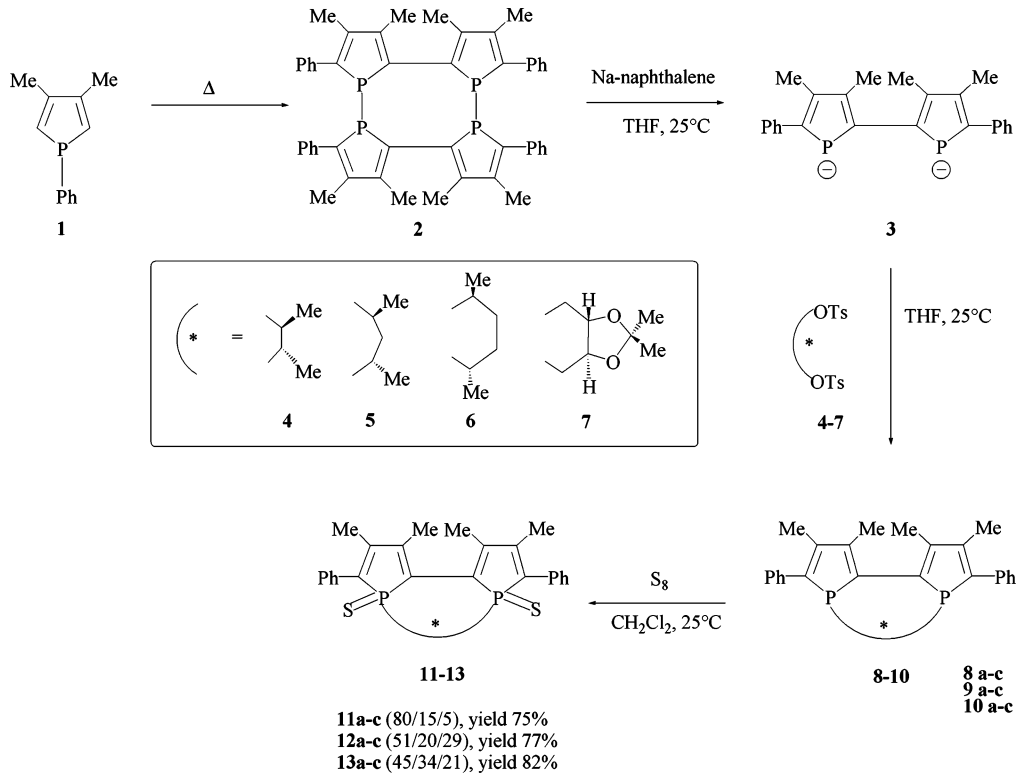

to diastereo- and enantiopure 2,2′-biphosphole Pd-complexes.[9]

Here, we report a convenient procedure for the preparation of various stereochemically dynamic 2,2′-biphospholes by asymmetric alkylation of 2,2′-biphospholyl anion with enantiomerically pure ditosylates. Since the use of these chirally flexible diphosphanes in asymmetric catalysis relies on the slow interconversion of chiral configurations, the isomerization process was studied. These diphosphanes became stereorigid as disulfide derivatives, allowing structural and stereochemistry studies by X-ray diffraction analysis and molecular modeling. We have also examined the dynamic resolution of these stereochemically dynamic 2,2′-biphospholes by coordination to transition metals such as palladium(II) and platinum(II). Their use in palladium-catalyzed asymmetric allylic substitution is also reported.

Synthesis of 2,2′-Biphosphole Ligands. The strategy used to access resolved 2,2′-biphosphole compounds is based on a two-step chirality control process: (1) partial chirality control in order to keep some degree of freedom; (2) total chirality control by enantioselective coordination on a metal center.

The axial and central chiralities of the 2,2′-biphosphole framework can be controlled by introducing a chiral linker, such as a chiral carbon chain, between the two phosphorus atoms. We have investigated the asymmetric alkylation of the 2,2-biphosphole dianion with enantiomerically pure diol ditosylates. The synthetic pathway involved three steps starting from 1-phenyl-2,3-dimethylphosphole **1**.[10] In the first step, pyrolysis of phosphole **1** using the procedure previously described by Mathey and et al.[11] gave the tetraphosphole **2** (Scheme 1). In the next step, cleavage of the two phosphorus−phosphorus bonds in **2** using sodium naph-

Table 1. Selected Geometrical Parameters within the Biphosphole Framework

compound code	P−C−C−P torsion angle (deg)	dihedral angle between phosphole rings (deg)
R[*Sp,Sp,Rc,Rc*]-**12a**	−79.7(3)	71.50(6)
R[*Rp,Sp,Rc,Rc*]-**12b**	−52.1(3)	51.92(8)
S[*Rp,Rp,Rc,Rc*]-**12c**	89.2(9)	79.6(2)
S[*Rp,Sp,Rc,Rc*]-**13a**	50.4(2)	52.75(6)
R[*Sp,Sp,Rc,Rc*]-**13c**	−81.9(3)	81.3(1)
S[*Rp,Rp,Rc,Rc*]-**13b**	81.7(3)	81.1(1)
R[*Sp,Sp,Sc,Sc*]-**11a**	−55.4(2)	59.8(6)
S[*Rp,Rp,Sc,Sc*]-**11c**	84.4(3) [mean value]	87.9(1) [mean value]
R[*Sp,Rp,Sc,Sc*]-**11b**	−23(2) [mean value]	33(1) [mean value]
R[*Rp,Sp,Sc,Sc*]-**15**	−8.4(3)	20.2(2)
S[*Rp,Sp,Rc,Rc*]-**17**	5.9(2)	29.8(9)

Table 2. Torsion Angles (deg) within the Chiral Chain for Compounds 11a, 11b, and 11c

torsion angle	**11a**	**11c**	**11b**
C(111)−C(1)−C(2)−C(3)	169.2(2)	−163.3(4) [−160.6(4)]	−172(2)[−165(2)]
C(1)−C(2)−C(3)−C(311)	168.5(2)	28.7(5) [28.4(6)]	53(3)[62(3)]

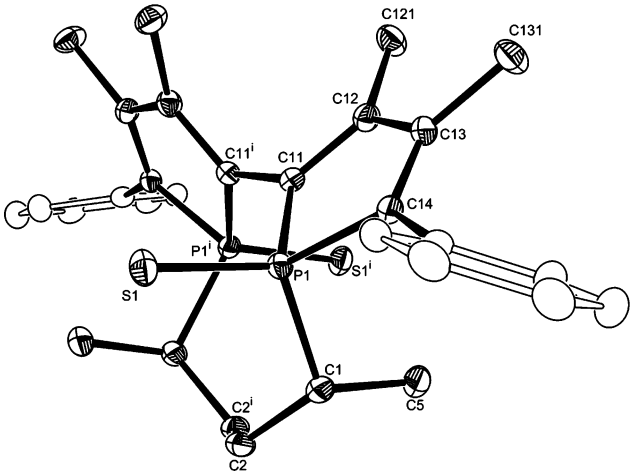

Figure 1. Molecular view of *R*[*Sp,Sp,Rc,Rc*]-**12a** with atom labeling. Ellipsoids represent 30% probability [symmetry code: (i) $-y, -x, -z + 1/2$]. Selected bond distances (Å): P(1)−S(1) 1.9597(6); P(1)−C(1) 1.840(2); P(1)−C(11) 1.801(2); P(1)−C(14) 1.818(2).

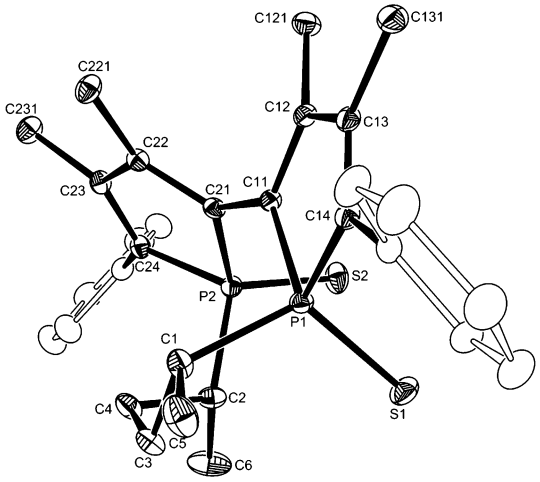

Figure 2. Molecular view of *R*[*Rp,Sp,Rc,Rc*]-**12b** with atom labeling. Ellipsoids represent 30% probability. Selected bond distances (Å): P(1)−S(1) 1.9553(7); P(1)−C(1) 1.846(2); P(1)−C(11) 1.825(2); P(1)−C(14) 1.818(2); P(2)−S(2) 1.9405(8); P(2)−C(2) 1.827(2); P(2)−C(21) 1.815(2); P(2)−C(24) 1.809(2).

thalene led to the 2,2′-biphospholyl anion **3**. Then, we have investigated the asymmetric alkylation of **3** in high dilution conditions using various enantiomerically pure diol ditosylates **4**−**7**. (2*R*,3*R*)-2,3-Butaneditosylate **4** could not react with **3** possibly because of the too short C_2-chain to bridge the two phosphorus atoms. In contrast, ditosylates **5**−**7** reacted with **3** to afford 2,2′-biphospholes **8**−**10**, respectively, as a mixture of three diastereoisomers in each case (Scheme 1).

To facilitate the separation and characterization of these diastereoisomers, 2,2′-biphospholes **8**−**10** were converted into more air-stable disulfide derivatives. 2,2′-Biphosphole disulfides **11**−**13** were quantitatively obtained by sulfuration of **8**−**10**, respectively, a process that occurs with retention of configuration at phosphorus[12] (Scheme 1). The three diastereoisomers **a**, **b**, and **c** of each disulfide compound could be isolated by column chromatography and characterized by ^{1}H, ^{13}C, and ^{31}P NMR spectroscopy, mass spectroscopy, and X-ray diffraction studies.

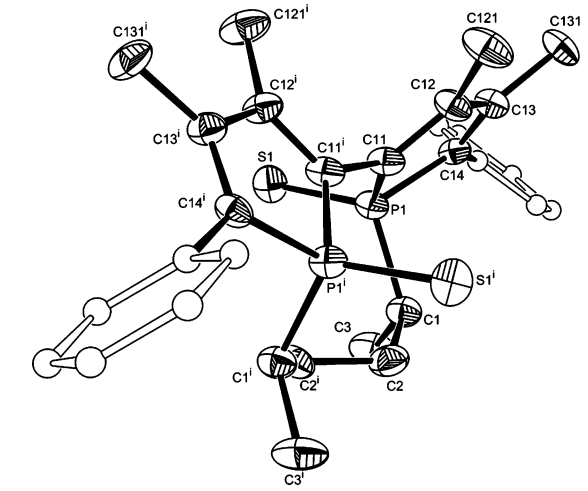

Figure 3. Molecular view of *S*[*Rp,Rp,Rc,Rc*]-**12c** with atom labeling. Ellipsoids represent 30% probability. Selected bond distances (Å): P(1)−S(1) 1.946(2); P(1)−C(1) 1.846(6); P(1)−C(11) 1.784(6); P(1)−C(14) 1.799(5).

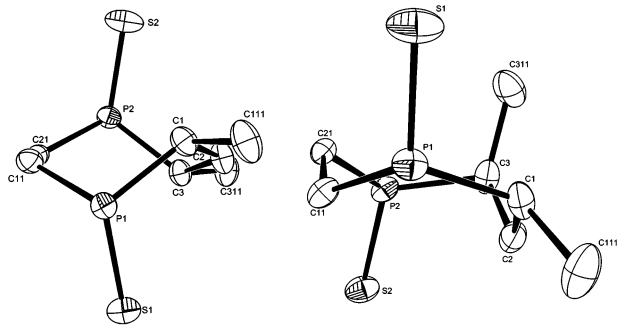

11a **11c**

Figure 4. View of the seven-membered rings for compounds *R*[*Sp,Sp,Sc,Sc*]-**11a** and *S*[*Rp,Rp,Sc,Sc*]-**11c** emphasizing the difference of conformation for the chiral chain.

Structural and Stereochemical Studies. The ORTEP views of the S-protected ligands **12a**−**c** emphasizing the axial chirality of the biphosphole framework are represented in Figures 1 to 3. The other structures related to ligands **11a**−**c** and **13a**−**c** are deposited in the Supporting Information. For all structures, the distances and angles within the phosphole rings are identical within experimental error and in good agreement with reported structures.[7,13] As shown in Table 1, the P−C−C−P torsion angle and the dihedral angle between the two phosphole rings are strongly dependent on the relative chirality of the phosphorus atoms. Indeed, the absolute value of this torsion angle varies from 79.7° to 89.2° in the case of the two phosphorus having the same chirality, whereas this value varies from 50.4 to 52.1 when the two phosphorus have

(9) Ortega, C.; Gouygou, M.; Daran, J.-C. *Chem. Commun.* **2003**, 1154−1155.
(10) Breque, A.; Mathey, F.; Savignac, P. *Synthesis* **1981**, 983−985.
(11) Laporte, F.; Mercier, F.; Ricard, L.; Mathey, F. *J. Am. Chem. Soc.* **1994**, *116*, 3306−3311.
(12) (a) McEven, W. E. *Top. Phosphorus Chem.* **1965**, *2*, 1. (b) Gallaher, M. J.; Jenkins, J. D. *Top. Stereochem.* **1969**, *3*, 1.
(13) Tissot, O.; Hydrio, J.; Gouygou, M.; Dallemer, F.; Daran, J.-C.; Balavoine, G. G. A. *Tetrahedron* **2000**, *56*, 85−93. Hydrio, J.; Gouygou, M.; Dallemer, F.; Balavoine, G. G. A.; Daran, J.-C. *Eur. J. Org. Chem.* **2002**, 675−685.

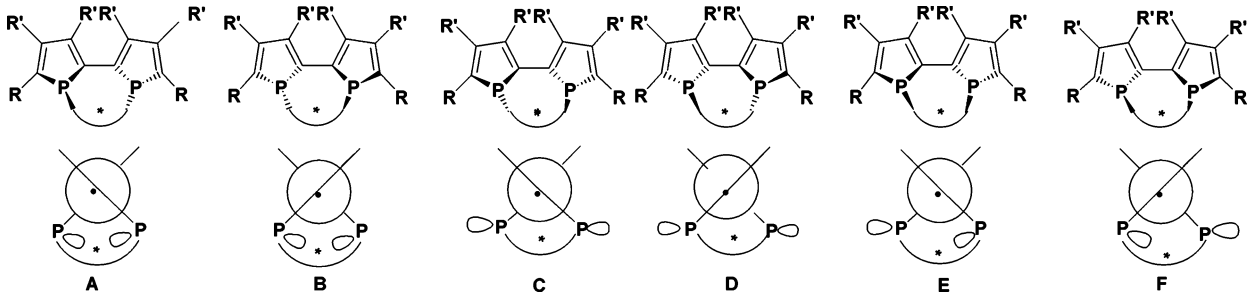

Figure 5. Different stereoisomers of 2,2′-biphosphole that possess two chiral centers and one chiral axis; each stereoisomer is also represented in a Newman projection along the axis of the C−C linking the phosphole rings.

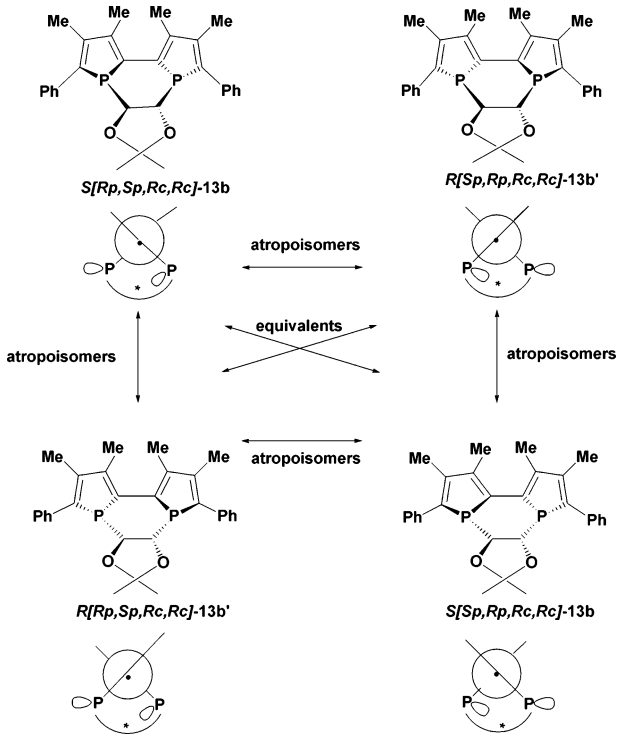

Figure 6. Different atropoisomers of 2,2′-biphosphole **13b**.

opposite configuration. There is however one exception for compound **11a**, for which the torsion angle is −55.4(2)°, although the two phosphorus have the same chirality. In that case, the influence of the conformation of the chiral chain overcomes the chirality on phosphorus. Indeed, if we consider the conformation of the chain in compounds **11a** and **11c** as shown in Table 2, the torsion angles clearly indicate that the position of the methyl groups with respect to the C(1)···C(3) direction is *cis* in the case of **11a** and *trans* for **11c**. The *cis* conformation results in the P atoms being on the opposite side to the plane containing the chiral chain (Figure 4), thus restraining the dihedral angle between the phosphole rings. In compound **11b**, a similar calculation reveals a *trans* conformation for the chiral chain, but here the low value of the P−C−C−P torsion angle is related to the opposite configuration of the phosphorus atoms.

These structural determinations unambiguously established the relative configuration of both the central and the axial elements of chirality of the 2,2′-biphosphole framework. The different possibilities of combining axial and central chiralities in 2,2′-biphosphole are depicted in Figure 5. This stereochemical analysis shows the occurrence of six diastereoisomers.

Only three diastereoisomers are obtained by introduction of a chiral bridge between the two phosphorus atoms of the 2,2′-biphosphole framework. The stereoisomer C is obtained for compounds **11c**, **12c**, and **13b**, D for compounds **11a**, **12a**, and **13c**, E for compound **13a**, and F for compound **11b** and **12b**. These results clearly indicate that the introduction of a short chiral linker, such as a C3- or C4-chain, between the two phosphorus atoms prevents the formation of A and B forms to favor the C and D and E or F configurations (Figure 5). C and D stereoisomers are always isolated, whereas either the E or F isomer is obtained.

The E and F stereoisomers could be considered as two atropoisomers, as illustrated in Figure 6. Conformational analysis of the rotation process around the C−C bond linking the two phosphole rings was performed on 2,2′-biphospholes **13** by molecular mechanics calculations. According to these calculations, the *S*[*Rp,Sp,Rc,Rc*]-**13b** isomer (E form) is energetically more favored than the *R*[*Rp,Sp,Rc,Rc*]-**13b′** isomer (F form); the difference in energy between these two atropoisomers is 23 kcal·mol^{-1}. Moreover, these calculations agree with experimental observations since the three isolated isomers **13a**, **13b**, and **13c** are located approximatively at the same energy level (differences in energy are within the range 5 to 8 kcal·mol^{-1}).

Since the sulfur addition to trivalent phosphorus compounds proceeds with retention of configuration,[12] these results suggest that the configurations determined for the 2,2′-biphosphole disulfide would be identical for the corresponding free 2,2′-biphosphole ligand.

Scheme 2. Stereoselective Desulfuration of [*Sp,Sp,Sc,Sc*]-(+)-3,3′,4,4′-Tetramethyl-5,5′-diphenyl-1,1′-(pentane-2,4-diyl)-2,2′-biphospholyl 1,1′-disulfide, 11a

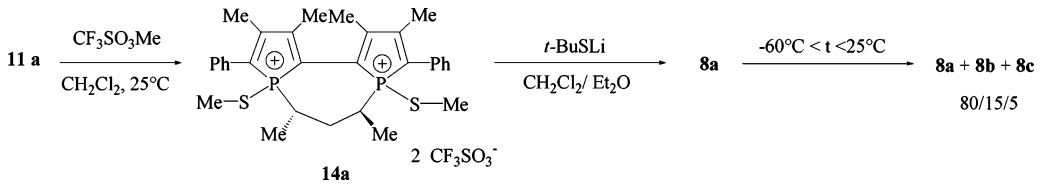

Finally, as three diastereoisomers are obtained among the six expected, the chiral controllers have induced partial chirality control of the 2,2′-biphosphole framework.

In addition a good carbon-to-phosphorus induction has been observed in particular in the case of compound **8** (**11**), in which the original *R,R* chirality of the enantiomerically pure diol ditosylate induces the preferred *S,S* stereochemistry of the phosphorus atoms.[14] The decrease in induction observed from **8** (**11**) to **9** (**12**) is probably due to an increase of the carbon chain length. In the case of compound **10** (**13**), the moderate carbon-to-phosphorus induction could be assigned to a longer carbon linker associated with stereogenic centers farther away from the phosphorus atoms.

Isomerization Process. To study the isomerization process in these stereochemically dynamic 2,2′-biphospholes, we have investigated the desulfurization of compounds **11a**, **11b**, and **11c** by using a fully stereoselective method[15] that affords at low temperature chiral phosphines with retention of configuration. *R*[*Sp,Sp,Sc,Sc*]-**11a** reacted with methyltrifluoromethane sulfonate to give compound **14a** ($\delta^{31}P = 60.5$) in quantitative yield (Scheme 2). Then, the reaction with *tert*-butyllithium sulfide at −60 °C led to the formation of *R*[*Sp,Sp,Sc,Sc*]-**8a** as major product along with *R*[*Sp,Rp,Sc,Sc*]-**8b** and *S*[*Rp,Rp,Sc,Sc*]-**8c** as minors products, as indicated by ^{31}P NMR. This is indicative of an isomerization process taking place at −60 °C. The ratio **8a**:**8b**:**8c** of 80/15/5 was then obtained at 25 °C.

On the other hand, *S*[*Rp,Rp,Sc,Sc*]-**11c** was quantitatively transformed into **14c** ($\delta^{31}P = 65.35$). Treatment of **14c** with *t*-BuSLi at −70 °C afforded a mixture of **8c**, **8b**, and **8a**, as evidenced by ^{31}P NMR analysis (Figure 7). The isomerization process was monitored by ^{31}P NMR from −70 to 25 °C (Figure 7). These data are consistent with an interconversion of **8c** to **8a** via **8b**.

Since the chiral bridge in 2,2-biphosphole compounds prevents the formation of A and B forms (Figure 5), the only possible pathway for this isomerization requires a phosphorus inversion[16] inducing an atropoinversion as illustrated in Figure 8.[17]

Palladium and Platinum Complexes. Before engaging in asymmetric catalysis, the coordination chemistry of these new ligands was studied. Initial complexing experiments were performed with palladium(II) and platinum(II) precursors.

The reaction of **8a**−**c** in CH_2Cl_2 at room temperature with 1 equiv of $[PdCl_2(CH_3CN)_2]$ led to complete consumption of the ligand in 1 h at room temperature to afford [$PdCl_2$(2,2′-biphosphole)] **15** (90%) and an unidentified product (10%)[18] (Scheme 3). Complex *R*[*Rp,Sp,Sc,Sc*]-**15** could be isolated in a pure form and characterized by ^1H, ^{13}C, and ^{31}P NMR spectroscopy, mass spectroscopy, and X-ray diffraction studies. Two palladium complexes were also obtained in the same

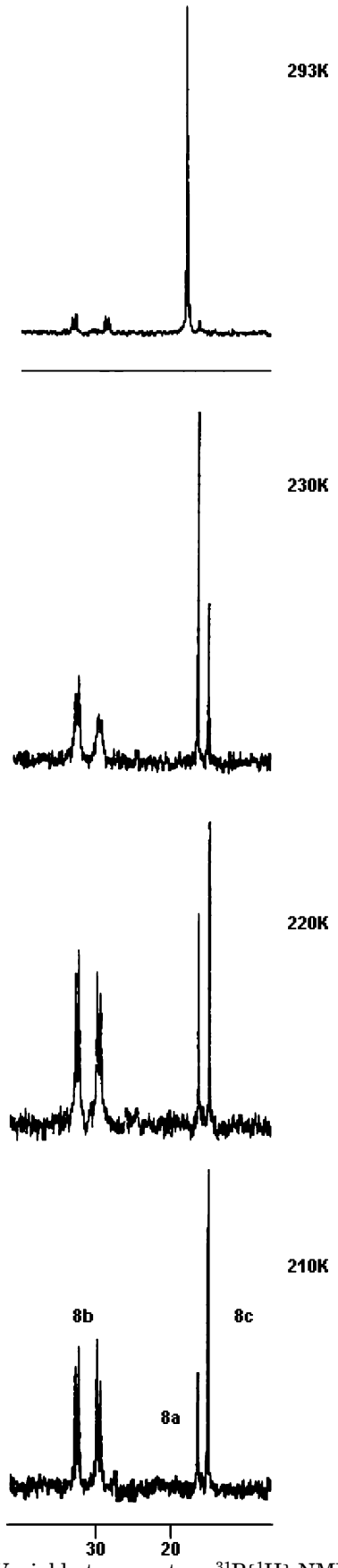

Figure 7. Variable-temperature $^{31}P\{^1H\}$ NMR spectra of desulfurization of **11c**.

(14) Nucleophilic subtitution on carbon resulted in inversion of configuration in the case of compounds **8** (**11**) and **9** (**12**).

(15) (a) Omelanczuk, J.; Mikolajczyk, M. *J. Am. Chem. Soc.* **1979**, *101*, 7292. (b) Omelanczuk, J.; Perlikowska, W.; Mikolajczyk, M. *J. Chem. Soc., Chem. Commun.* **1980**, 24.

(16) In 2,2′-biphosphole, the inversion barrier for the pyramidal phosphorus is reduced, relative to that in phosphines, as a result of the increase in aromatic character of the phosphorus in the transition state; see ref 7.

(17) The driving force of this isomerization process should be the phosphorus inversion. No interconversion between **a**, **b**, and **c** occurred even at +90 °C in toluene according to NMR studies. In 2,2-biphosphole disulfides the pyramidal inversion at phosphorus is suppressed, as the lone pairs are masked by sulfur.

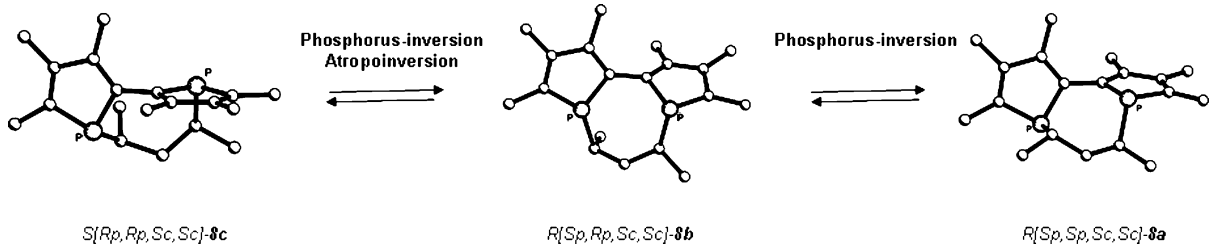

Figure 8. Isomerization process in the stereochemically dynamic 2,2-biphospholes.

Scheme 3. Synthesis of 2,2′-Biphosphole Metal Complexes

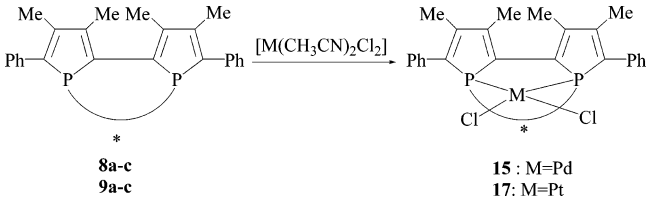

conditions with the ligands **9a**−**c**, but they could not be separated and identified.

With the $[PtCl_2(CH_3CN)_2]$ precursor, the reaction of the ligands **8a**−**c**, **9a**−**c**, and **10a**−**c** was complete in 3 days at room temperature in dichloromethane and only affords [$PtCl_2$(2,2′-biphosphole)] **16**, **17**, and **18**, respectively, as indicated by ^{1}H, ^{13}C, and ^{31}P NMR spectroscopy and mass spectroscopy. The structure of the *S*[*Rp,Sp,Rc,Rc*]-**17** complex was determined by X-ray diffraction analysis. All these complexes could be quantitatively obtained in 3 h by refluxing in dichloromethane the ligands **8a**−**c**, **9a**−**c**, and **10a**−**c** and the $[PtCl_2(CH_3CN)_2]$ precursor.

Molecular views of complexes *R*[*Rp,Sp,Sc,Sc*]-**15** and *S*[*Rp,Sp,Rc,Rc*]-**17** are shown in Figures 9 and 10. In both compounds, the coordination around the metal is square planar. The X-ray structure of **15**[9] and **17** indicates that only the [*Rp,Sp*] configuration of 2,2-biphosphole is complexed to the metal center. The axial chirality of the 2,2-biphosphole framework is reduced upon complexing. Indeed, owing to the strain induced by chelating on the metal, the P(1)−C(11)−C(21)−P(2) torsion angle, (**15**: −8.4(3)°, **17**: 5.9 (2)°) is drastically reduced from the values observed in free ligands (Table 1). The strain induced by the coordination is also reflected by the larger difference observed between torsion and dihedral angles. The phosphole rings are not only twisted along the C−C bond linking the rings but are also bent with respect to each other to help the phosphorus atoms to accommodate the coordination on the metal atom. It is interesting to point out that this deformation is much larger with the platinum complex **17**.

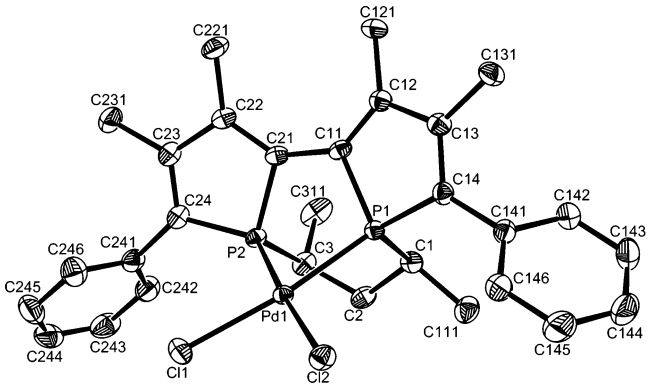

Figure 9. Molecular view of *R*[*Rp,Sp,Sc,Sc*]-**15** with atom-labeling scheme. Ellipsoids represent 50% probability. Selected bond distances (Å): Pd(1)−P(1) 2.2735(6); Pd(1)−P(2) 2.2479(6); Pd(1)−Cl(1) 2.3381(7); Pd(1)−Cl(2) 2.3514-(6); P(1)−C(1) 1.867(3); P(1)−C(11) 1.820(2); P(1)−C(14) 1.803(3); P(2)−C(3) 1.845(3); P(2)−C(21) 1.803(3); P(2)−C(24) 1.796(3).

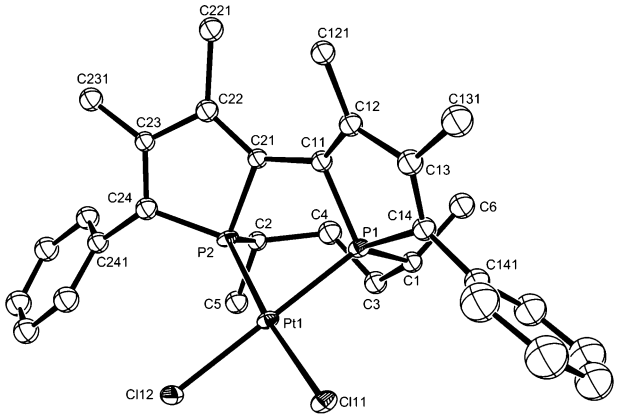

Figure 10. Molecular view of *S*[*Rp,Sp,Rc,Rc*]-**17** with atom-labeling scheme. Ellipsoids represent 30% probability. Selected bond distances (Å): Pt(1)−P(1) 2.239(4); Pt(1)−P(2) 2.247(4); Pt(1)−Cl(1) 2.348(4); Pt(1)−Cl(2) 2.350-(4); P(1)−C(1) 1.80(2); P(1)−C(11) 1.82(2); P(1)−C(14) 1.78-(2); P(2)−C(2) 1.87(2); P(2)−C(21) 1.82(2); P(2)−C(24) 1.77(2).

These results show that reaction of the diastereoisomeric mixture of equilibrating 2,2-biphosphole with $[MCl_2(CH_3CN)_2]$ resulted in a dynamic resolution mixture to give diastereo- and enantiopure Pd- or Pt-complexes.

Asymmetric Pd-Allylic Substitution. As a preliminary evaluation of the catalytic properties of the chiral ligands **8** and **10**, we have explored the palladium-catalyzed asymmetric allylic substitution reaction[19] (Scheme 3). Thus, the reaction of 1,3-diphenylprop-2-enyl acetate **19** with the anion of dimethyl malonate in the presence of $[Pd(C_3H_5)Cl]_2$ (1.5 mol %) and the chiral ligands **8** and **10** (3 mol %) provided the expected allylic substitution product **20** (Scheme 4) in high yields and moderate enantioselectivities. The results are summarized in Table 3.

This reaction occurred with 33% and 34% ee for **8** and **10**, respectively (entries 1, 3), with high activities in both

(18) This unidentified product is a palladium complex with four diastereotopic phosphorus having opposite phosphorus configurations [*Rp,Sp*] according to ^{31}P NMR (δp 53.2 (d) , δp 51.2(d), J_{PP} 3.25; δp 52.9(s), δp 50.9(s)).

(19) Trost, B. M.; Van Vranken, D. L. *Chem. Rev.* **1996**, *96*, 395−422.

Scheme 4. Allylic Substitution Reaction

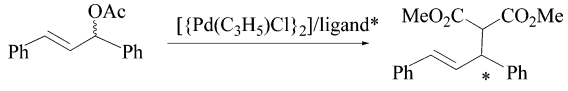

19 **20**

Table 3. Results of Asymmetric Allylic Substitution Reaction of 1,3-Diphenylprop-2-enyl Acetate with the Anion of Dimethyl Malonate

entry	ligand	base	solvent	reaction time	yield[b]	ee% of **18**[c] (config)[d]
1	**8** (3%)	BSA/AcOK	CH_2Cl_2	30 min	96%	33 (*S*)
2	**8** (3%)	BSA/AcOK	THF	5 h	66%	15 (*S*)
3	**10** (3%)	BSA/AcOK	CH_2Cl_2	1 h	93%	34 (*S*)

[a] Reaction conditions: 1 mmol of (*E*)-1,3-diphenylprop-2-enyl acetate, 3 mmol of dimethylmalonate with 3% palladium as $[PdCl(allyl)]_2$ at RT. The complete conversion was observed by ^{1}H NMR expect for the entries 1 and 3. [b] Isolated yield. [c] Determined by ^{1}H NMR using the chiral shift reagent Eu(hfc)$_3$. [d] Determined on the basis of the sign of the specific rotation of the product.

cases with complete conversion after 30−60 min at room temperature using CH_2Cl_2 as solvent and *N*,*O*-bis-(trimethylsilyl)acetamide (BSA)/AcOK as base. The use of THF as solvent decreased the rate of the reaction (entry 2), as the complete conversion was not observed after 5 h, and affected the enantioselectivity (15%).

These results show that palladium-catalyzed allylic substitution of 1,3-diphenylprop-2-enyl acetate with the anion of dimethyl malonate can be achieved with ligands **8** and **10** with high activities but still moderate enantioselectivities (up to 34% ee) in comparison with the best values obtained with the well-known chirally rigid diphosphines.[19]

Conclusions

A new and convenient preparation of stereodynamic 2,2′-biphosphole ligands and a highly and practical transformation to diastereo- and enantiopure complexes have been achieved. Furthermore, the direct use of these stereodynamic ligands in palladium-catalyzed asymmetric allylic substitution has been demonstrated. Catalyst optimization through the modification of the chiral linker represents a viable approach currently being developed.

Experimental Section

General Procedures. All reactions were carried out under dry argon by using Schlenk glassware and vacuum line techniques. Solvents were freshly distilled from standard drying agents. ^{1}H, ^{13}C{^{1}H, ^{31}P}, and ^{31}P{^{1}H} ^{195}Pt NMR spectra were recorded on Bruker WMX 400 and AV 500 instruments. Mass spectra were obtained on a Nermag R10-10 instrument. Elemental analyses were performed by the "Service d'Analyse du Laboratoire de Chimie de Coordination" at Toulouse. Optical rotations were measured with a Perkin-Elmer 241 polarimeter.

1-Phenyl-3,4-dimethylphosphole **1**,[10] tetraphosphole **2**,[11] dianion **3**,[11] and enantiomerically pure diol ditosylates (*R,R*)-**4**, (*R,R*)-**5**, (*S,S*)-**6**, and (*R,R*)-**7**[20] were prepared as described in the literature.

General Procedure for Compounds 8, 9, and 10. In a Schlenk tube, naphthalene (0.02 g, 1.88 mmol) was stirred with an excess of sodium (∼0.5 g) in dry THF (6 mL) until the solution became green. Solid tetramer **1** (400 mg, 0.54 mmol) was then added slowly in portions. The reaction mixture turned red and was stirred until it became green again (∼2 h). This solution of dianion **2** and a THF solution (6 mL) of ditosylate (1.08 mmol) were transferred dropwise by cannula at the same time into an other Schlenk containing 200 mL of dry THF, and the reaction mixture was stirred for 16 h at room temperature. After evaporation to dryness, the resulting residue was extracted with small portions of pentane. The combined pentane extracts were filtered through Celite, and the solvents were evaporated to give crude compound. This compound was purified by filtration on alumina under argon using a mixture of 95/5 pentane/dichloromethane as solvent.

8. ^{31}P NMR ($CDCl_3$): δ 16 (**8c**), 18 (**8a**), 27(d, P1), 31(d, P2), *J*P1,P2 = 42 Hz (**8b**).

9. ^{31}P NMR ($CDCl_3$): δ 21.49 (s, P1), 22.7 (s, P2) (**9b**), 22.25 (**9a**), 33.66 (**9c**).

10. ^{31}P NMR ($CDCl_3$): δ 0.48 (d, P1), 9.06 (d, P2), *J*P1,P2 = 8.0 Hz (**10a**), 6.13 (**10c**), 8.31 (**10b**).

General Procedure for Compounds 11, 12, and 13. Sulfur (2 equiv) was added to a solution of crude 2,2′-biphosphole compound in dichloromethane (30 mL), and the reaction mixture was stirred overnight at room temperature. After evaporation to dryness, the mixture was chromatographed on silica gel.

***R*[*Sp,Sp,Sc,Sc*]-(+)-3,3′,4,4′-Tetramethyl-5,5′diphenyl-1,1′-(pentane-2,4-diyl)-2,2′-biphospho-lyl 1,1′-Disulfide, 11a.** Eluent: pentane/dichloromethane, 40/60. Yellow solid (yield = 53%). Mp = 298−301 °C. ^{1}H NMR ($CDCl_3$): δ 0.77 (dd, *J*H,P = 17.8 Hz, *J*H,H = 6.9 Hz, 6H, C*H*3-CH), 1.78 (m, 1H, CH2), 1.85 (m, 1H, CH2), 2.07 (dd, *J*H,P = 2.5 Hz, *J*H,P = 2.3 Hz, 6H, C*H*3-C-C), 2.10 (d, *J*H,P = 2.6 Hz, 6H, C*H*3-C-CPh), 3.13 (m, 2H, CH-P), 7.36 (m, 6H, Ph), 7.68 (m, 4H, Ph). ^{13}C NMR ($CDCl_3$): δ 15.73 (d, *J*C,P = 12.9 Hz, *C*H3-C-CPh), 16.07 (dd, *J*C,P = 12.5 Hz, *J*C,P = 2.2 Hz, *C*H3-C-C), 17.55 (t, *J*C,P = 1.73 Hz, *C*H3-CH), 32.30 (dd, *J*C,P = 45.6 Hz, *J*C,P = 2.6 Hz, CH), 39.09 (t, *J*C,P = 2.94 Hz, CH_2), 128.37 (s, Ph) 128.88 (s, Ph) 129.42 (t, *J*C,P = 2.54 Hz, C_{ortho}), 130.95 (dd, JC,P = 76.9 Hz, *J*C,P = 12.4 Hz, Ph-*C*-P), 133.50 (dd, *J*C,P = 73.4 Hz, *J*C,P = 2.0 Hz, C-Ph), 135.34 (d, *J*C,P = 10.4 Hz, C_{ipso}), 148.69 (dd, *J*C,P = 23.9 Hz, *J*C,P = 2.2 Hz, CH_3-*C*-C), 148.79 (dd, *J*C,P = 22.9 Hz, *J*C,P = 2.2 Hz, CH_3-*C*-C-Ph). ^{31}P NMR ($CDCl_3$): δ 61.03. $[\alpha]_D$ +155.6 (CH_2Cl_2, *c* 0.5). MS (DCI, NH_3) *m/z*: (%) 507 (100%) $[M + H]^+$. Anal. Calcd for $C_{29}H_{32}P_2S_2$ (507.15): C 68.78, H 6.36, S 12.64. Found**:** C 68.05, H 6.24, S 13.28. Crystals suitable for X-ray analysis were obtained by slow evaporation of a dichloromethane solution.

***R*[*Sp,Rp,Sc,Sc*]-(+)-3,3′,4,4′-Tetramethyl-5,5′diphenyl-1,1′-(pentane-2,4-diyl)-2,2′-biphospho-lyl 1,1′-Disulfide, 11b.** Eluent: diethyl ether. Yellow solid. Yield = 10%. ^{1}H NMR ($CDCl_3$): δ 0.96 (d, *J*H,H = 10 Hz, 3H, C*H*3-CHP(1)), 1.00 (d, *J*H,H = 5 Hz, 3H, C*H*3-CHP(2)), 1.71 (m, 2H, CH−P), 2.04 (d, *J*H,P = 10 Hz, 6H, C*H*3-C-C), 2.08 (d, *J*H,P = 2.5 Hz, 6H, C*H*3-C-CPh), 2.12 (m, 2H, CH2), 7.35 (m, 2H, Ph), 7.40 (m, 4H, Ph) 7.64 (m, 4H, Ph). ^{13}C NMR ($CDCl_3$): δ 15.11(d, *J*C,P = 12.5 Hz, *C*H3-C-CPh), 17.41 (s, *C*H3−CH), 18.65 (d, *J*C,P = 11.2 Hz, *C*H3-C-C), 22.64 (s, CH_2), 29.66 (s, CH), 127.95 (d, *J*C,P = 7.5 Hz, C-P), 128.47 (s, C_{para}), 128.89 (s, C_{meta}), 129.10 (s, C_{ortho}), 134.24 (d, *J*C,P = 11.2 Hz, Ph-*C*-P), 136.66 (s, C_{ipso}), 146.50 (s, CH_3-*C*-C), 148.20 (s, CH_3-*C*-C-Ph). ^{31}P NMR ($CDCl_3$): δ 63.3 P(1), 67.3 P(2). $[\alpha]_D$ +417.1 (CH_2Cl_2, *c* 0.14). MS (DCI, NH_3) *m/z*: (%) 507 (100%) $[M + H]^+$. Crystals suitable for X-ray analysis were obtained by slow evaporation of a diethyl ether solution.

***S*[*Rp,Rp,Sc,Sc*]-(+)-3,3′,4,4′-Tetramethyl-5,5′diphenyl-1,1′-(pentane-2,4-diyl)-2,2′-biphospho-lyl 1,1′-Disulfide, 11c.** Eluent: pentane/dichloromethane, 45/55. Yellow solid (yield = 4%). Mp = 178−180 °C. ^{1}H NMR ($CDCl_3$): δ 1.00 (dd, *J*H,P = 18.5 Hz, *J*H,H = 7.4 Hz, 6H, C*H*3-CH), 2.15 (dd, *J*H,P = 2.2 Hz, *J*H,P = 0.9 Hz, 6H, C*H*3-C-C), 2.18 (m, 2H, CH2),

(20) Bakos, J.; Tóth, I.; Heil, B.; Markó, L. *J. Organomet. Chem.* **1985**, *279*, 23−29.

2.26 (dd, *J*H,P = 3.2 Hz, *J*H,P = 1.9 Hz, 6H,C*H*3-C-CPh), 2.37 (m, 2H, CH-P), 7.34 (m, 2H, Ph), 7.42 (m, 4H, Ph) 7.70 (m, 4H, Ph). ^{13}C NMR ($CDCl_3$): δ 15.70 (dd, *J*C,P = 14.0 Hz, *J*C,P = 1.0 Hz, *C*H3-C-CPh), 16.48 (s, *C*H3-CH), 16.82 (dd, *J*C,P = 13.2 Hz, *J*C,P = 3.6 Hz, *C*H3-C-C), 32.01 (t, *J*C,P = 1.8 Hz, CH_2), 38.16 (d, *J*C,P = 44.2 Hz, CH), 125.75 (dd, *J*C,P = 74.3 Hz, *J*C,P = 9.6 Hz,C−P), 128.37 (s, C_{para}), 128.99 (s, C_{meta}), 129.30 (t, *J*C,P = 2.8 Hz, C_{ortho}), 133.63 (dd, *J*C,P = 76.9 Hz, *J*C,P = 12.4 Hz, Ph-*C*-P), 134.98 (dd, *J*C,P = 12.4 Hz, *J*C,P = 2.7 Hz, C_{ipso}), 149.50 (dd, *J*C,P = 23.2 Hz, *J*C,P = 4.1 Hz, CH_3-*C*-C), 153.00 (dd, *J*C,P = 24.2 Hz, *J*C,P = 6.4 Hz, CH_3-*C*-C-Ph). ^{31}P NMR ($CDCl_3$): δ 67.34. $[\alpha]_D$ +356.6 (CH_2Cl_2, *c* 0.5). MS (DCI, NH_3) *m/z*: (%) 507 (100%) $[M + H]^+$. Anal. Calcd for $C_{29}H_{32}P_2S_2$ (507.15): C 68.78, H 6.36, S 12.64. Found**:** C 68.69, H 6.89, S 11.70. Crystals suitable for X-ray analysis were obtained by slow evaporation of a dichloromethane solution.

12a, **12b**, and **12c**, which could not be isolated in a pure form, have been partly characterized.

***R*[*Sp,Sp,Rc,Rc*]-3,3′,4,4′-Tetramethyl-5,5′diphenyl-1,1′-(hexane-2,5-diyl)-2,2′-biphospholyl 1,1′-Disulfide, 12a.** Pentane/dichloromethane: 30/70. Yellow solid. ^{1}H NMR ($CDCl_3$): δ 0.86 (m, 6H, C*H*3-CH), 2.06 (d, *J*H,P = 2.3 Hz, 6H, C*H*3-C-C), 2.13 (d, *J*H,P = 2.2 Hz, 6H, C*H*3-C-CPh), 7.36 (m, 6H, Ph), 7.65 (m, 4H, Ph). ^{31}P NMR ($CDCl_3$): δ 70.9. Crystals suitable for X-ray analysis were obtained by slow evaporation of a dichloromethane solution.

***R*[*Rp,Sp,Rc,Rc*]-3,3′,4,4′-Tetramethyl-5,5′diphenyl-1,1′-(hexane-2,5-diyl)-2,2′-biphospholyl 1,1′-Disulfide, 12b.** Eluent: ether. Yellow solid. ^{1}H NMR ($CDCl_3$): δ 0.85 (m, 6H, C*H*3-CH), 1.83 (m, 2H, CH2), 1.97 (d, *J*H,P = 2.3 Hz, 6H, C*H*3-C-C), 2.07 (d, *J*H,P = 2.4 Hz, 6H, C*H*3-C-CPh), 7.30 (m, 6H, Ph), 7.66 (m, 4H, Ph). ^{31}P NMR ($CDCl_3$): δ 64.67 P(1), 64.73 P(2). MS (DCI, NH_3) *m/z*: (%) 521 (100%) $[M + H]^+$. Crystals suitable for X-ray analysis were obtained by slow evaporation of a dichloromethane solution.

***S*[*Rp,Rp,Rc,Rc*]-3,3′,4,4′-Tetramethyl-5,5′diphenyl-1,1′-(hexane-2,5-diyl)-2,2′-biphospholyl 1,1′-Disulfide, 12c.** Pentane/dichloromethane: 50/50. Yellow solid. ^{1}H NMR ($CDCl_3$): δ 0.81 (m, 6H, C*H*3-CH), 2.07 (d, *J*H,P = 2.2 Hz, 6H, C*H*3-C-C), 2.17 (d, *J*H,P = 2.4 Hz, 6H, C*H*3-C-CPh), 7.34 (m, 6H, Ph), 7.60 (m, 4H, Ph). ^{31}P NMR ($CDCl_3$): δ 70.1. MS (DCI, NH_3) *m/z*: (%) 521 (100%) $[M + H]^+$. Crystals suitable for X-ray analysis were obtained by slow evaporation of a dichloromethane solution.

***S*[*Rp,Sp,Rc,Rc*]-(−)-3,3′,4,4′-Tetramethyl-5,5′diphenyl-1,1′-(2,3-*O*-isopropylidene-2,3-dihydroxybutane-1,4-diyl)-2,2′-biphospholyl 1,1′-Disulfide, 13a.** Eluent: pentane/dichloromethane, 40/60 (yellow solid). Yield = 32%. Mp = 215−220 °C. ^{1}H NMR ($CDCl_3$): δ 1.30 (s, 6H, C*H*3-CO), 1.63 (m, 1H, CH2-P(1)), 2.00 (s, 3H, C*H*3-C-C), 2.03 (s, 3H, C*H*3-C-CPh), 2.07 (s, 3H, C*H*3-C-C), 2.08 (s, 3H, C*H*3-C-CPh), 2.58 (m, 1H, CH2-P(2)), 2.68 (m, 1H, CH2-P(1)), 3.05 (m, 1H, C*H*-CH2-P(2)), 3.67 (m, 1H, CH2-P_2), 4.41 (m, 1H, C*H*-CH2-P(1)), 7.33−7.53 (m, 10H, Ph). ^{13}C NMR ($CDCl_3$): δ 15.51 (d, *J*C,P-(1) = 13.3 Hz, *C*H3-C-CPh), 15.57 (d, *J*C,P(2) = 12.2 Hz, *C*H3-C-CPh), 17.31 (dd, *J*C,P(2) = 12.1 Hz, *J*C,P(1) = 1.5 Hz, *C*H3-C-C), 17.97 (d, *J*C,P(2) = 12.67 Hz, *C*H3-C-C), 27.15 (s, $(CH_3)_2C$), 27.24 (s, $(CH_3)_2C$), 28.45 (d, *J*C,P(1) = 47.3 Hz, CH_2-P(1)), 34.31 (d, *J*C,P(2) = 45.5 Hz, CH_2-P(2)), 76.67 (d, *J*C,P-(2) = 2.3 Hz, *C*H-CH_2-P(2)), 78.06 (dd, *J*C,P(1) = 5.3 Hz, *J*C,P(2) = 2.9 Hz, *C*H-CH_2-P(1)), 107.82 (s, $(CH_3)_2C$), 127.59 (dd, *J*C,P(2) = 76.7 Hz, *J*C,P(1) = 12.6 Hz, *C*-P(2)), 128.82 (s, C_{para}), 128.87 (s, C_{para}), 129.12 (s, C_{meta}), 129.15 (s, C_{ortho}), 129.29 (s, C_{meta}), 130.00 (s, C_{ortho}), 130.92 (dd, JC,P(1) = 79.0 Hz, *J*C,P-(2) = 13.5 Hz, *C*-P(1)), 132.41 (d, *J*C,P(2) = 12.0 Hz, C_{ipso}-P(2)), 132.68 (d, *J*C,P(1) = 12.0 Hz, C_{ipso}-P(1)), 135.93 (d, *J*C,P(1) = 78.5 Hz, Ph-*C*-P(1)), 136.93 (d, *J*C,P(2) = 77.5 Hz, Ph-*C*-P(2)), 146.88 (d, *J*C,P(2) = 22.1 Hz, CH_3-*C*-C-Ph), 148.14 (d, *J*C,P-(1) = 24.1 Hz, CH_3-*C*-C-Ph), 150.23 (dd, *J*C,P(1) = 24.7 Hz, *J*C,P(2) = 9.5 Hz, CH_3-*C*-C-P(1)), 151.27 (dd, *J*C,P(2) = 23.1 Hz, *J*C,P(2) = 10.0 Hz, CH_3-*C*-C-P(2)). ^{31}P NMR ($CDCl_3$): δ 55.36 P(2), 51.05 P(1). $[\alpha]_D$ −127.6 (CH_2Cl_2, *c* 0.5). MS (DCI, NH_3) *m/z*: (%) 565 (100%) $[M + H]^+$. Anal. Calcd for $C_{31}H_{34}O_2P_2S_2$ (564.15): C 65.96, H 6.03, S 11.34. Found: C 66.20, H 6.41, S 9.06. Crystals suitable for X-ray analysis were obtained by slow evaporation of a dichloromethane solution.

***S*[*Rp,Rp,Rc,Rc*]-(+)-3,3′,4,4′-Tetramethyl-5,5′diphenyl-1,1′-(2,3-*O*-isopropylidene-2,3-dihydroxybutane-1,4-diyl)-2,2′-biphospholyl 1,1′-Disulfide, 13b.** Eluent: pentane/dichloromethane, 35/75. Yellow solid (yield = 20%). Mp = 244−245 °C. ^{1}H NMR ($CDCl_3$): δ 1.31 (s, 6H, CH3-CO), 2.09 (dd, *J*H,P = 3.1 Hz, *J*H,P = 2.3 Hz, 6H, CH_3), 2.13 (m, 2H, CH2−P), 2.17 (dd, *J*H,P = 2.5 Hz, *J*H,P = 0.7 Hz, 6H, CH_3), 2.35 (dd, *J*H,P = 15.3 Hz, *J*H,H = 14.9 Hz, 2H, CH2-P), 4.40 (m, 2H, C*H*-CH2-P), 7.41 (m, 6H, Ph), 7.61 (m, 4H, Ph). ^{13}C NMR ($CDCl_3$): δ 15.60 (d, *J*C,P = 6.7 Hz, *C*H3-C-CPh), 15.95 (dd, *J*C,P = 12.7 Hz, *J*C,P = 2.8 Hz, *C*H3-C-C), 27.23 (s, $(CH_3)_2C$), 31.51 (d, *J*C,P = 46.5 Hz, CH_2-P), 76.8 (dd, *J*C,P = 5.3 Hz, *J*C,P = 1.2 Hz *C*H-CH_2-P), 107.59 (s, $(CH_3)_2C$), 127.54 (dd, *J*C,P = 79.9 Hz, *J*C,P = 11.9 Hz, *C*-P), 129.06 (d, *J*C,P = 1.6 Hz, C_{meta}), 129.25 (d, *J*C,P = 0.7 Hz C_{para}), 129.50 (dd, *J*C,P = 4.6 Hz, *J*C,P = 0.8 Hz C_{ortho}), 132.62 (dd, *J*C,P = 11.1 Hz, *J*C,P = 1.5 Hz, C_{ipso}), 135.49 (dd, *J*C,P = 79.2 Hz, *J*C,P = 2.9 Hz, *C*-Ph), 147.23 (dd, *J*C,P = 23.9 Hz, *J*C,P = 2.5 Hz, CH_3-*C*-C-Ph), 152.36 (dd, *J*C,P = 25.8 Hz, *J*C,P = 7.7 Hz, CH_3-*C*-C-P). ^{31}P NMR ($CDCl_3$): δ 54.93. $[\alpha]_D$ +43.9 (CH_2Cl_2, *c* 0.5). MS (DCI, NH_3) *m/z*: (%) 565 (100%) $[M + H]^+$. Anal. Calcd for $C_{31}H_{34}O_2P_2S_2$ (564.15): C 65.96, H 6.03, S 11.34. Found: C 65.56, H 6.56, S 9.12. Crystals suitable for X-ray analysis were obtained by slow evaporation of a dichloromethane solution.

***R*[*Sp,Sp,Rc,Rc*]-(+)-(−)-3,3′,4,4′-Tetramethyl-5,5′diphenyl-1,1′-(2,3-*O*-isopropylidene-2,3-dihydroxybutane-1,4-diyl)-2,2′-biphospholyl 1,1′-Disulfide, 13c.** Eluent: pentane/dichloromethane, 30/70. Yellow solid (yield = 14%). Mp = 252−255 °C. ^{1}H NMR ($CDCl_3$): δ 1.37 (s, 6H, CH3-CO), 2.13 (m, 12H, CH_3), 2.34 (ABX, *J*H,P = 15.0 Hz, *J*H,H = 15.0 Hz, *J*H,H = 7.0 Hz, 2H,CH2-P), 2.70 (ABX, *J*H,P = 15.0 Hz, *J*H,H = 15.0 Hz, *J*H,H = 4.5 Hz, 2H, CH2-P), 4.75 (m, 2H, C*H*-CH2-P), 7.40 (m, 6H, Ph), 7.60 (m, 4H, Ph). ^{13}C NMR ($CDCl_3$): δ 15.44 (d, *J*C,P = 13.0 Hz, *C*H3-C-CPh), 16.59 (dd, *J*C,P = 12.4 Hz, *J*C,P = 2.0 Hz, *C*H3-C-C), 27.87 (s, $(CH_3)_2C$), 34.25 (d, *J*C,P = 45.3 Hz, CH_2-P), 76.65 (d, *J*C,P = 4.3 Hz, *C*H-CH_2-P), 109.19 (s, $(CH_3)_2C$), 127.35 (dd, *J*C,P = 77.9 Hz, *J*C,P = 11.9 Hz, *C*-P), 128.94 (d, *J*C,P = 1.5 Hz, C_{meta}), 129.22 (s, C_{para}), 129.70 (d, *J*C,P = 5.0 Hz, C_{ortho}), 132.70 (dd, *J*C,P = 11.3 Hz, *J*C,P = 0.9 Hz, C_{ipso}), 136.94 (dd, *J*C,P = 77.0 Hz, *J*C,P = 2.9 Hz, *C*-Ph), 146.17 (dd, *J*C,P = 23.3 Hz, *J*C,P = 2.3 Hz, CH_3-*C*-C-Ph), 153.55 (dd, *J*C,P = 25.65 Hz, *J*C,P = 7.5 Hz, CH_3-*C*-C-P). ^{31}P NMR ($CDCl_3$): δ 53.37. $[\alpha]_D$ −8.4 (CH_2Cl_2, *c* 0.5). MS (DCI, NH_3) *m/z*: (%) 565 (100%) $[M + H]^+$. Anal. Calcd for $C_{31}H_{34}O_2P_2S_2$ (564.15): C 65.96, H 6.03, S 11.34. Found: C 65.74, H 6.00, S 10.20. Crystals suitable for X-ray analysis were obtained by slow evaporation of a dichloromethane solution.

General Procedure for the Desulfurization. To a solution of 2,2′-biphosphole (0.26 mmol) in dichloromethane (5 mL) was added dropwise CF_3SO_3Me (0.058 mL, 0.52 mmol). After 1 h of stirring, the resulting suspension was evaporated to dryness and the 2,2′-biphosphonium salt was washed with small portions of pentane. A solution of this salt in dichloromethane (5 mL) was added dropwise to a solution of *t*-BuSLi, resulting from treatment at −40 °C of 2-methyl-2-propane thiol (0.645 mL, 0.57 mmol) in ether (4 mL) with *n*-buthyllithium (0.208 mL, 0.52 mmol, 2.5 M in hexane). The resulting mixture was stirred for 15 min at −78 °C and for 2 h at RT and then evaporated to dryness. The resulting residue was extracted with small portions of pentane. The combined pentane phases were washed with water, dried over $MgSO_4$, and evaporated to give crude compound in 95% yield.

***R*[*Rp,Sp,Sc,Sc*]-(+)-3,3′,4,4′-Tetramethyl-5,5′diphenyl-1,1′-(pentane-2,4-diyl)-2,2′-biphospholyl-*P,P*′-dichloro-**

palladium(II), 15. To a solution of compound **8** (40 mg, 0.09 mmol) in CH_2Cl_2 (10 mL) was added $[PdCl_2(CH_3CN)_2]$ (27.46 mg, 0.10 mmol) in CH_2Cl_2 (10 mL). The resulting solution was stirred 16 h at room temperature, filtered through a 0.45 μm PTFE filter, and then concentrated under reduced pressure to give a solid residue. This resulting solid was dissolved in a small amount of CH_2Cl_2 and precipitated with a large excess of pentane. After filtration, the red solid obtained was dried under vacuum (50 mg, 90%). ^{1}H NMR ($CDCl_3$): δ 0.75 (dd, *J*H,P2 = 14.2 Hz, *J*H,H = 7.0 Hz, 3H, C*H*3-CH), 0.93 (dd, *J*H,-P1 = 16.4 Hz, *J*H,H = 7.2 Hz, 3H, C*H*3-CH), 2.22 (d, *J*H,P1 = 2.4 Hz, 3H, C*H*3-C-C), 2.26 (d, *J*H,P2 = 2.4 Hz, 3H, C*H*3-C-C), 2.44 (s, 3H, C*H*3-C-CPh), 2.47 (s, 3H, C*H*3-C-CPh), 7.32−7.49 (m, 6H, $H_{meta,para}$), 7.90 (m, 4H, H_{ortho}). ^{13}C NMR ($CDCl_3$): δ 12.68 (d, *J*C,P = 6.2 Hz, *C*H3-CHP(1)), 17.73 (dd, *J*C,P = 10.3 Hz, *J*C,P = 18.6 Hz, *C*H3-C-C), 19.05 (s, *C*H3-CHP(2)), 19.56 (dd, *J*C,P = 10.3 Hz, *J*C,P = 41.1 Hz, *C*H3-C-C), 29.72 (dd, *J*C,P = 4.5 Hz, *J*C,P = 20.7 Hz, CHP(1)), 34.18 (dd, *J*C,P = 7.0 Hz, *J*C,P = 19.3 Hz, CH P(2)), 43.79 (t, *J*C,P = 7.5 Hz, CH_2), 128.74 (d, *J*C,P = 14.7 Hz, CH_p), 129.66 (d, *J*C,P = 24.4 Hz, CH_m), 131.4 (d, JC,P = 5.2 Hz, CH_o), 133.19 (d, *J*C,P = 12.6 Hz, C_{ipso}), 132.36 (d, *J*C,P = 4.7 Hz,CHo), 135.26 (m, C−P), 141.96 (d, *J*C,P = 51.8 Hz, Ph-*C*), 143.59 (dd, *J*C,P = 11.35 Hz, *J*C,P = 46 Hz, CH_3-*C*−), 155.06 (dd, *J*C,P = 16.62 Hz, *J*C,P = 16.58 Hz, CH_3-*C*). ^{31}P NMR ($CDCl_3$): δ 76.4 (s, P1), 84.5 (s, P2). $[\alpha]_D$ +144 (CH_2Cl_2, *c* 0.15). MS (FAB, MNBA matrix) *m/z*: 583[M − Cl]$^+$ (100%), 547[M$^+$ − 2Cl]$^+$ (60%). Crystals suitable for X-ray analysis were obtained by slow evaporation of a CH_2Cl_2 solution.

General Procedure for Platinum Complexes 16, 17, and 18. To a solution of ligand **8**, **9**, or **10** (0.19 mmol) in CH_2Cl_2 (20 mL) was added slowly $[PtCl_2(CH_3CN)_2]$ (69 mg, 0.19 mmol). The resulting solution was refluxed 3 h, then allowed to warm to room temperature and concentrated under reduced pressure to give a solid residue. This yellow solid was dissolved in a small amount of CH_2Cl_2 and precipitated with a large excess of pentane. After filtration, the solid was washed with small portions of pentane and dried under vacuum.

(−)-3,3′,4,4′-Tetramethyl-5,5′diphenyl-1,1′-(pentane-2,4-diyl)-2,2′-biphospholyl-*P,P′*-dichloroplatinum(II), 16. Yellow solid (yield = 92%). ^{1}H NMR ($CDCl_3$): δ 0.79 (dd, *J*H,P2 = 25.0 Hz, *J*H,H = 5.0 Hz, 3H, C*H*3-CHP2), 0.96 (dd, *J*H,P1 = 25.0 Hz, *J*H,H = 5.0 Hz, 3H, C*H*3-CHP1), 1.50 (m, 2H, C*H*-P), 2.20 (d, *J*H,P1 = 5.0 Hz, 3H, C*H*3-C-C), 2.29 (d, *J*H,P2 = 5.0 Hz, 3H, C*H*3-C-C), 2.42 (s, 3H, C*H*3-C-CPh), 2.47 (s, 3H, C*H*3-C-CPh), 2.53 (m, 2H, −CH_2-CHP), 7.33−7.37 (m, 2H, H_{para}), 7.44−7.48 (m, 4H, H_{meta}), 7.85 (d, *J*H,H = 5.0 Hz, 2H, H_{ortho}), 7.98 (d, *J*H,H = 5.0 Hz,2H, H′$_{ortho}$). ^{13}C NMR ($CDCl_3$): δ 13.55 (d, *J*C,P1 = 3.7 Hz, *C*H3-CHP(1)), 17.14 (d, *J*C,P1 = 11.2 Hz, *C*H3−C−C), 17.23 (d, *J*C,P1 = 11.2 Hz, *C*H3-C-C), 18.33 (s, *C*H3-CHP(2)), 18.75 (d, *J*C,P = 10.0 Hz, *C*H3-C-C), 19.15 (d, *J*C,P = 11.2 Hz, *C*H3-C-C), 27.98 (dd, *J*C,P = 2.5 Hz, *J*C,P = 26.2 Hz, CHP(1)), 32.89 (dd, *J*C,P = 3.7 Hz, *J*C,P = 28.7 Hz, CHP(2)), 43.53 (s, CH_2), 128.24 (d, *J*C,P = 6.25 Hz, CH_p), 128.68 (s, CH_m), 128.89 (s, CH_m), 130.73 (d, *J*C,P = 3.7 Hz,CH_o), 131.79 (d, *J*C,P = 3.7 Hz,CH_o), 133.16 (d, *J*C,P = 12.5 Hz, C_{ipso}), 133.94 (d, *J*C,P = 11.2 Hz, C-P), 141.58 (m, Ph-*C*), 143.21 (m, CH_3-*C*−), 154.69 (m, CH_3-*C*). ^{31}P NMR ($CDCl_3$): δ 53.86 (dt, *J*P1,P2 = 12.1 Hz, *J*P1,Pt = 3193.6 Hz, P1), 58.41 (t, *J*P2,Pt = 3193.6 Hz, P2). ^{195}Pt NMR ($CDCl_3$): δ −4232.24 (t, *J*Pt,P = 3167.7 Hz). $[\alpha]_D$ −96.1 (CH_2Cl_2, *c* 0.23). MS (FAB, MNBA matrix) *m/z*: 673[M − Cl]$^+$.

***S*[*Rp,Sp,Rc,Rc*]-(−)-3,3′,4,4′-Tetramethyl-5,5′diphenyl-1,1′-(hexane-2,5-diyl)-2,2′-biphospholyl-*P,P′*-dichloroplatinum(II), 17.** Yellow solid (yield = 91%). ^{1}H NMR ($CDCl_3$): δ 0.91 (dd, *J*H,P2 = 15.0 Hz, *J*H,H = 15.0 Hz, 3H, C*H*3-CH), 1.07 (dd, *J*H,P1 = 20.0 Hz, *J*H,H = 15.0 Hz, 3H, C*H*3-CH), 1.74 (m, 4H, −CH_2-CHP), 1.96 (d, *J*H,P1 = 1.92 Hz, 3H, C*H*3-C-C), 2.12 (d, *J*H,P2 = 1.92 Hz, 3H, C*H*3-C-C), 2.34 (s, 3H, C*H*3-C-CPh), 2.37 (s, 3H, C*H*3-C-CPh), 7.29−7.37 (m, 2H, H_{para}), 7.39−7.43 (m, 4H, H_{meta}), 7.65 (m, 2H, H_{ortho}), 7.71 (m, 2H, H′$_{ortho}$). ^{13}C NMR ($CDCl_3$): δ 12.53 (d, *J*C,P1 = 2.86 Hz, *C*H3-CHP(1)), 15.88 (d, *J*C,P2 = 2.51 Hz, *C*H3-CHP(2)), 16.31 (d, *J*C,P1 = 10.1 Hz, *C*H3-C-C), 16.42 (d, *J*C,P1 = 10.1 Hz, *C*H3-C-C), 19.45 (d, *J*C,P = 11.3 Hz, *C*H3-C-C), 20.05 (dd, *J*C,P = 10.1 Hz, *C*H3-C-C), 27.33 (d, *J*C,P = 2.5 Hz, *J*C,P = 26.7 Hz, CHP(1)), 29.84 (s, CHP(2)), 33.63 (d, *J*C,P = 26.4 Hz, CH_2), 37.08 (d, *J*C,P = 33.96 Hz, CH_2), 128.21 (m, CH_p), 128.39 (m, CH_m), 131.06 (d, *J*C,P = 2.5 Hz,CH_o), 131.65 (d, *J*C,P = 2.5 Hz,CH_o), 133.54 (d, *J*C,P = 11.3 Hz C_{ipso}), 134.02 (d, *J*C,P = 11.3 Hz, C-P), 143.65 (m, Ph-*C*), 145.98 (m, CH_3-*C*−), 153.65 (d, *J*C,P = 17.5 Hz, CH_3-*C*). ^{31}P NMR ($CDCl_3$): δ 50.24 (dt, *J*P1,P2 = 6.1 Hz, *J*P1,Pt = 3265.0 Hz, P1), 62.00 (t, *J*P2,Pt = 3265.0 Hz, P2). ^{195}Pt NMR ($CDCl_3$): δ −4209.73 (t, *J*Pt,P = 3270.0 Hz). $[\alpha]_D$ −124.6 (CH_2Cl_2, *c* 0.15). MS (FAB, MNBA matrix) *m/z*: 687[M − Cl]$^+$. Crystals suitable for X-ray analysis were obtained by slow evaporation of a dichloromethane solution.

(+)-3,3′,4,4′-Tetramethyl-5,5′diphenyl-1,1′-(2,3-*O*-isopropylidene-2,3-dihydroxybutane-1,4-diyl)-2,2′-biphospholyl-*P,P′*-dichloroplatinum(II), 18. Yellow solid (yield = 94%). ^{1}H NMR ($CDCl_3$): δ 1.34 (m, 6H, C*H*3-CO), 1.76 (m, 1H, CH2-P(1)), 2.09 (d, 3H, C*H*3-C-C), 2.10 (d, 3H, C*H*3-C-C), 2.34 (s, 3H, C*H*3-C-CPh), 2.45 (s, 3H, C*H*3-C-CPh), 2.65 (m, 2H, CH2-P(2)), 3.06 (m, 1H, CH2-P(1)), 3.75 (m, 1H, C*H*-CH2-P(2)), 5.03 (m, 1H, C*H*-CH2-P(1)), 7.37−7.65 (m, 10H, Ph). ^{13}C NMR ($CDCl_3$): δ 16.54 (d, *J*C,P(1) = 15.0 Hz, *C*H3-C-CPh), 16.59 (d, *J*C,P(2) = 16.2 Hz, *C*H3-C-CPh), 19.35 (d, *J*C,P(1) = 11.2 Hz, *C*H3-C-C), 20.15 (d, *J*C,P(2) = 11.2 Hz, *C*H3-C-C), 26.77 (s, $(CH_3)_2$C), 26.94 (s, $(CH_3)_2$C), 33.09 (d, *J*C,P(2) = 27.5 Hz, CH_2-P(2)), 36.23 (d, *J*C,P(1) = 30.0 Hz, CH_2-P(1)), 78.04 (d, *J*C,P(1) = 10 Hz, *C*H-CH_2-P(1)), 78.68 (d, *J*C,P(2) = 3.7 Hz, *C*H-CH_2-P(2)), 109.27 (s, $(CH_3)_2C$), 128.56 (s, C_{para}), 128.63 (s, C_{para}), 130.56 (d, *J*C,P = 3.7 Hz, C_{meta}), 130.85 (s, *C*-P(2)), 131.61 (d, C_{ortho}), 131.73 (d, *J*C,P(1) = 3.7 Hz, *C*-P(1)), 132.10 (d, *J*C,P(2) = 11.2 Hz, C_{ipso}-P(2)), 133.08 (s, C_{ipso}-P(1)), 135.20 (s, Ph-*C*-P(1)), 136.75 (s, Ph-*C*-P(2)), 144.69 (m, CH_3-*C*-C-Ph), 145.38 (s, CH_3-*C*-C-Ph), 153.11 (s, CH_3-*C*-C-P(1)), 153.22 (s, CH_3-*C*-C-P(2)). ^{31}P NMR ($CDCl_3$): δ 34.55 (dt, *J*P1,P2 = 4.05 Hz, *J*P1,Pt = 3231.9 Hz, P1), 37.36 (t, *J*P2,Pt = 3231.9 Hz, P2). ^{195}Pt NMR ($CDCl_3$): δ −4144.98 (t, *J*Pt,P = 3238.9 Hz). $[\alpha]_D$ +227.7 (CH_2Cl_2, *c* 0.18). MS (FAB, MNBA matrix) *m/z*: 731[M − Cl]$^+$.

General Procedure for Palladium-Catalyzed Allylic Substitution. A mixture of ligand **8** or **10**, 1,3-diphenylprop-2-enyl acetate (0.413 g, 1.63 mmol), and $[(Pd(C_3H_5)Cl)]_2$ (3 mg, 0.03 mmol) in dry solvent (20 mL) was stirred at room temperature for 2 h. To the resulting solution were added dimethyl malonate (0.374 mL, 3.25 mmol), a small amount of potassium acetate, and BSA (0.300 mL, 3.25 mmol). The reaction was carried out at room temperature and monitored by TLC for disappearance of acetate. After complete reaction, the resulting mixture was diluted with diethyl ether (5 mL) and quenched with a saturated aqueous solution of ammonium chloride (5 mL). The aqueous phase was extracted with Et_2O, and the combined organic layers were dried over sodium sulfate, filtered, and evaporated. The conversion was calculated from the crude reaction mixture by ^{1}H NMR spectroscopy. Subsequent purification by chromatography on silica eluting with ethyl acetate/pentane (15/85) afforded the product as a white solid. The enantiomeric excess was determined by ^{1}H NMR using the chiral shift reagent Eu(hfc)$_3$.

X-ray Structure Determination. A single crystal of each compound was mounted under inert perfluoropolyether at the tip of a glass fiber and cooled in the cryostream of either an Oxford-Diffraction XCALIBUR CCD diffractometer for **12b** or a Stoe IPDS diffractometer for **12a**, **12c**, **13a**, **13b**, and **16**. Data were collected using monochromatic Mo Kα radiation (λ = 0.71073).

Table 4. Crystal Data and Structure Refinement

	12b	12a	12c	11b
empirical formula	$C_{30}H_{34}P_2S_2$	$C_{30}H_{34}P_2S_2$	$C_{30}H_{34}P_2S_2$	$C_{29}H_{27}P_2S_3$
fw	520.63	520.63	520.63	506.61
temp, K	180(2)	180(2)	180(2)	180(2)
wavelength, Å	0.71073	0.71073	0.71073	0.71073
cryst syst	triclinic	tetragonal	tetragonal	triclinic
space group	$P\bar{1}$	$P4_12_12$	$P4_32_12$	$P\bar{1}$
a, Å	7.5069(7)	8.2848(7)	9.3019(6)	8.937(2)
b, Å	8.4348(8)	8.2848(7)	9.3019(6)	10.911(2)
c, Å	11.3734(10)	39.289(3)	31.650(3)	15.546(4)
α, deg	78.136(7)	90.0	90.0	82.55(3)
β, deg	83.429(7)	90.0	90.0	73.47(3)
γ, deg	82.062(8)	90.0	90.0	67.38(3)
volume, Å3	695.26(11)	2696.8(4)	2738.6(4)	1341.1(6)
Z	1	4	4	2
density (calcd), Mg/m^3	1.243	1.282	1.263	1.255
abs coeff, mm^{-1}	0.324	0.334	0.329	0.334
F(000)	276	1104	1104	536
cryst size, mm^3	0.401 × 0.334 × 0.221	0.55 × 0.31 × 0.25	0.36 × 0.28 × 0.008	0.425 × 0.15 × 0.025
θ range, deg	3.17 to 28.28	2.51 to 24.21	2.28 to 26.14	2.42 to 23.25
no. of reflns collected	6110	20 655	24 612	8682
no. of indep reflns [R(int)]	4374 (0.0131)	2166 (0.0472)	2726 (0.2224)	6302 (0.1570)
completeness, %,	99.2	99.3	99.6	91.1
abs corr	multiscan	none	analytical	empirical (DIFABS)
max., min. transmn	0.9247, 0.8729		0.9974, 0.9042	0.984 and 0.858
refinement method	F^2	F^2	F^2	F^2
no. of data/restraints/params	4374/3/313	2166/0/157	2726/0/159	6302/543/609
goodness-of-fit on F^2	1.118	1.067	0.905	0.906
final R indices [$I > 2\sigma(I)$]	R1 = 0.0293, wR2 = 0.0792	R1 = 0.0256, wR2 = 0.0636	R1 = 0.0545, wR2 = 0.1012	R1 = 0.1021, wR2 = 0.2666
R indices (all data)	R1 = 0.0306, wR2 = 0.0804	R1 = 0.0277, wR2 = 0.0656	R1 = 0.1717, wR2 = 0.1445	R1 = 0.2052, wR2 = 0.3242
abs struct param	−0.06(5)	0.00(9)	0.0(3)	not reliable
largest diff peak and hole, e Å^{-3}	0.326 and −0.237	0.149 and −0.161	0.376 and −0.491	0.417 and −0.396

	13a	13b(c)	16
empirical formula	$C_{31}H_{34}O_2P_2S_2$	$C_{124}H_{136}O_8P_8S_8$	$C_{30}H_{34}Cl_2P_2Pt$
fw	564.64	2258.57	722.50
temp, K	180(2)	180(2)	180(2)
wavelength, Å	0.71073	0.71073	0.71073
cryst syst	monoclinic	triclinic	orthorhombic
space group	$P2_1$	$P\bar{1}$	$P2_12_12_1$
a, Å	8.9710(16)	10.9358(9)	9.1281(9)
b, Å	14.164(2) Å	12.2064(11)	12.5047(10)
c, Å	11.563(2) Å	24.537(2)	24.788(2)
α, deg	90.0	93.484(11)	90.0
β, deg	93.02(2)	100.258(11)	90.0
γ, deg	90.0	112.899(9).	90.0
volume, Å^3	1467.3(4)	2938.2(5)	2829.5(4)
Z	2	1	4
density(calcd), Mg/m^3	1.278	1.276	1.696
abs coeff, mm^{-1}	0.317	0.317	5.279
F(000)	596	1192	1424
cryst size, mm^3	0.4 × 0.32 × 0.32	0.56 × 0.26 × 0.08	0.46 × 0.21 × 0.074
θ range, °	2.27 to 26.14	2.13 to 26.04.	2.31 to 26.00
no. of reflns collected	14704	29430	18049
no. of indep reflns [R(int)]	5718 (0.0517)	21206 (0.0481)	5482 (0.1005)
completeness, %,	98.1	92.8	99.2
abs corr	none	multiscan	multiscan
max., min. transmission		1.0 and 0.896	0.3639 and 0.2947
refinement method	F^2	F^2	F^2
data/restraints/parameters	5718/1/340	21206/1311/1376	5482/0/172
goodness-of-fit on F^2	1.042	0.938	1.124
final R indices [$I > 2\sigma(I)$]	R1 = 0.0264, wR2 = 0.0621	R1 = 0.0370, wR2 = 0.0795	R1 = 0.0749, wR2 = 0.1786
R indices (all data)	R1 = 0.0298, wR2 = 0.0639	R1 = 0.0514, wR2 = 0.0842	R1 = 0.0913, wR2 = 0.1851
absolute structure param	0.04(4)	0.04(4)	0.04(2)
largest diff peak and hole, e Å^{-3}	0.280 and −0.238	0.318 and −0.278	2.955 and −4.389

The structures were solved by direct methods (SIR97[21]) and refined by least-squares procedures on F^2 using SHELXL-97.[22] All H atoms attached to carbon were introduced in the calculation in idealized positions and treated as riding models. Absolute configuration was confirmed by the refinement of the Flack's enantiopole parameter[23] and careful examination of the sensitive reflections. In compound **13b**, which crystallized in the non-centrosymmetric $P1$ space group, there are four molecules in the unit cell. It is interesting to note that these four molecules correspond to two different diasteroisomers,

[*Sc,Sc,R,Sp,Sp*] and [*Sc,Sc,S,Rp,Rp*], related two by two. The data collected for compound **11b** were of very low quality owing to poor crystals. Although the results unambiguously reveal the opposite configuration of P atoms, the absolute configuration of the molecule could not be reliably determined and was then established from the known configuration of the chiral chain as defined in the structures of compounds **11a** and **11b**. The drawing of the molecules was realized with the help of ORTEP32.[24] Crystal data and refinement parameters are shown in Table 4.

Crystallographic data are also given as CIF files. This material is available free of charge via the Internet at http://pubs.acs.org.

(21) Altomare, A.; Burla, M. C.; Camalli, M.; Cascarano, G. L; Giacovazzo, C.; Guagliardi, A.; Moliterni, A. G. G.; Polidori, G.; Spagna, R. SIR97 a program for automatic solution of crystal structures by direct methods. *J. Appl. Crystallogr.* **1999**, *32*, 115.

(22) Sheldrick, G. M. *SHELXL 97*. Programm for crystal structure refinement; University of Göttingen: Germany, 1997.

(23) Flack, H. D. *Acta Crystallogr., Sect. A* **1983**, *39*, 876. Bernardinelli, G.; Flack, H. D. *Acta Crystallogr., Sect. A* **1985**, *41*, 500.

(24) Farrugia, L. J. ORTEP3 for Windows. *J. Appl. Crystallogr.* **1997**, *30*, 565.

Computational Details. The molecular mechanics calculations were carried out with the CAChe program using the MM2 force field. Molecular models **13a**, **13b**, and **13c** were created from the original crystal data. The molecular geometries were fully optimized until the energy change is less than 10^{-5} kcal/mol or until the molecule has been updated 3000 times. Conformational analysis of the rotation process around the C−C bond linking the two phospholes rings was carried out. A total of 721 points have been optimized to generate the potential energy surface.

Acknowledgment. We thank the Centre National de la Recherche Scientifique, the Ministère de l'Education Nationale, de la Recherche et de la Technologie (E.R.), UNAM (C.O.), and Demsol Programme of European Community (M.M.).

Supporting Information Available: Crystallographic data are also given as CIF files. This material is available free of charge via the Internet at http://pubs.acs.org.

OM0503646